Journal of Microbiology (2019) Vol. 57, No. 2, pp. 93–100
DOI 10.1007/s12275-019-9021-y
eISSN 1976-3794
pISSN 1225-8873

PROTOCOL

Determination of protein phosphorylation by polyacrylamide gel electrophoresis

Chang-Ro Lee[1]*, Young-Ha Park[2], Huitae Min[2], Yeon-Ran Kim[2], and Yeong-Jae Seok[2,3]*

[1]*Department of Biological Sciences, Myongji University, Yongin 17058, Republic of Korea*
[2]*School of Biological Sciences and Institute of Microbiology, Seoul National University, Seoul 08826, Republic of Korea*
[3]*Department of Biophysics and Chemical Biology, Seoul National University, Seoul 08826, Republic of Korea*

(Received Jan 11, 2019 / Accepted Jan 17, 2019)

Phosphorylation is the most important modification for protein regulation; it controls many signal transduction pathways in all organisms. While several tools to detect phosphorylated proteins have been developed to study a variety of basic cellular processes involving protein phosphorylation, these methods have several limitations. Many proteins exhibit a phosphorylation-dependent electrophoretic mobility shift (PDEMS) in sodium dodecyl sulfate-polyacrylamide gel electrophoresis (SDS-PAGE), and the molecular mechanism responsible for this phenomenon has been elucidated recently. The method for detecting phosphorylated proteins can be simplified by the application of the PDEMS. Herein, we present a novel simple method to detect protein phosphorylation, which is based on the construction of a variant protein displaying a PDEMS. The PDEMS of proteins is caused by the distribution of negatively charged amino acids around the phosphorylation site, i.e. an electrophoretic mobility shift (EMS)-related motif ($\Theta X_{1\text{-}3}\Theta X_{1\text{-}3}\Theta$, where Θ corresponds to an acidic or phosphorylated amino acid and X represents any amino acid). The EMS-related motif can be constructed by the introduction of a negative charge by phosphorylation; it results in the decreased binding of SDS to the proteins, consequently inducing the retardation of the mobility of the protein during SDS-PAGE. Based on these molecular analyses of the PDEMS, a protein with the EMS-related motif is designed and used to determine the *in vivo* phosphorylation state of the protein. This method may be used as a general strategy to easily measure the ratio of protein phosphorylation in cells.

*For correspondence. (C.R. Lee) E-mail: crlee@mju.ac.kr; Tel.: +82-31-330-6472 / (Y.J. Seok) E-mail: yjseok@snu.ac.kr; Tel.: +82-2-880-8827

Keywords: protein phosphorylation, electrophoretic mobility shift, SDS-PAGE, signal transduction, protein kinase

Overview

Protein phosphorylation is the most important post-translational modification; it modulates diverse cellular processes, such as gene expression, metabolism, cell cycle regulation, differentiation, and apoptosis (Cohen, 2002a; Manning *et al.*, 2002). To study these basic cellular processes involving protein phosphorylation, a technique to detect phosphorylated proteins is required. The technique used generally to quantitate the degree of protein phosphorylation is a radioisotope method, which can sensitively detect phosphorylated proteins using radioactive phosphate. However, this technique requires specific equipment and possesses a high risk of radioisotope contamination. To overcome these problems of the radioisotope technique, various other techniques have been developed, including western blot analysis using phospho-amino acid-specific antibodies (Inagaki *et al.*, 1997; Kaufmann *et al.*, 2001), quantitative mass spectrometry (Ji *et al.*, 2012), fluorescence method (Xu *et al.*, 2011; Bai *et al.*, 2013; Zhou *et al.*, 2013), colorimetric assay (Wang *et al.*, 2006), electrochemiluminescence (Zhao *et al.*, 2012), Raman spectroscopic assay (Li *et al.*, 2009), resonance light scattering (Wang *et al.*, 2005), Phos-tag SDS-PAGE technique (Kinoshita *et al.*, 2009, 2017), surface plasmon resonance imaging technique (Inamori *et al.*, 2005; Takeda *et al.*, 2010), and photoluminescence (Wang *et al.*, 2013). Among these methods, Western blot analysis using phospho-amino acid-specific antibodies is the most frequently used technique for the detection of protein phosphorylation at specific target sites. This method is a convenient and useful tool that determines site-specific phosphorylation both *in vitro* and *in vivo*. However, it is unsuitable for the estimation of the ratios of phosphorylation states. The Phos-tag SDS-PAGE method is a novel tool that detects protein phosphorylation on an SDS-PAGE gel, using an acrylamide-conjugated dinuclear metal complex of 1,3-bis[bis(pyridin-2-ylmethyl)amino]propan-2-olate, which reversibly captures a phospho-monoester dianion (Kinoshita *et al.*, 2009, 2017). Phosphorylated proteins exhibit a mobility shift during SDS-PAGE using a Phos-tag acrylamide gel, and are thus separated from their unphosphorylated forms (Kinoshita *et al.*, 2009). This method can easily measure quantitative ratios of phosphorylation states *in vivo*; however, the disadvantage of this method is that the Phos-

tag acrylamide gel is expensive.

A phosphorylation-dependent electrophoretic mobility shift (PDEMS) during SDS-PAGE in the absence of Phos-tag has often been observed in several prokaryotic and many eukaryotic proteins (Steiner *et al.*, 1990; Imbert *et al.*, 1996; Hogema *et al.*, 1998; Zhou *et al.*, 2000; Sasanuma *et al.*, 2008; Lee *et al.*, 2013a; Mir *et al.*, 2015; Alligand *et al.*, 2017; Heckman *et al.*, 2017). Because the *in vivo* phosphorylation state of proteins can be easily detected by the PDEMS, the elucidation of its molecular mechanism can have an important biological impact. We have recently analyzed the reason for the PDEMS and elucidated its precise mechanism (Lee *et al.*, 2013a, 2013b). Based on these analyses, we converted a protein not showing a PDEMS into one displaying a PDEMS via single-point mutagenesis, and successfully determined the *in vivo* phosphorylation state using this mutant protein (Lee *et al.*, 2013a). These results suggest that this simple method for the construction of a protein showing a PDEMS would be a useful tool for the detection of the phosphorylation state of proteins.

Applications

The analysis of the phosphorylation state of a protein provides a comprehensive understanding of the regulatory events of various biological processes. In bacteria, histidine kinases play a role in signal transduction across the cell membrane and can act as cellular receptors for signaling molecules in a way analogous to how tyrosine kinase receptors function in plants and animals (Zschiedrich *et al.*, 2016). Most histidine kinases exhibit autokinase, phosphotransferase and phosphatase activities. The phosphorylation state of intracellular proteins is regulated by the balanced control of the kinases and phosphatases. In animals, disruption of this balance could induce severe diseases, including inflammation, cancer, and Alzheimer's disease (Lee *et al.*, 2001; Cohen, 2002a, 2002b; Lee and Kim, 2017). Many protein kinase and phosphatase mutations have been related to cancer; thus, selective inhibitors (e.g. the approved drug Glivec) of protein kinases or phosphatases related to cancer could be used as drugs for the treatment of cancer (Cohen, 2002b). Alzheimer's disease is also associated with the perturbation of several protein kinases, which leads to the hyperphosphorylation of the microtubule-associated protein Tau (Lee *et al.*, 2001). The inhibition of protein kinases is considered a promising strategy for the treatment of Alzheimer's disease (Lee and Kim, 2017). Therefore, the development of effective tools for the determination of the phosphorylation state of a protein is important for understanding the molecular basis of diseases and for drug screening. The protocol described here provides a simple and inexpensive method for the determination of the *in vivo* phosphorylation state and the *in vitro* screening of inhibitors for a specific protein.

Methods

Construction of proteins displaying a PDEMS

Principle of the PDEMS : The phosphoenolpyruvate (PEP)-dependent phosphotransferase system (PTS) is one of the bacterial signal transduction systems in which the phosphate transfer proceeds sequentially from PEP to Enzyme I, HPr, Enzyme IIA (EIIA), EIIB, and finally the incoming sugar that is transported by a transmembrane protein, EIIC (Deutscher *et al.*, 2006). The glucose-specific enzyme IIA ($EIIA^{Glc}$) of *Escherichia coli* shows a PDEMS phenomenon when phosphorylated at its histidine site (H90) (Hogema *et al.*, 1998), whereas its paralog $EIIA^{Ntr}$ of the nitrogen PTS does not show a PDEMS when phosphorylated at its histidine site (H73) (Lee *et al.*, 2013a). Comparison of the amino acid sequences surrounding the phosphorylation sites of the two proteins provides an important clue for the reason behind the existence of the PDEMS in proteins. There are two negatively charged amino acids (E86 and D94) situated on both sides of the phosphorylation site of $EIIA^{Glc}$, whereas three negatively charged amino acids are clustered on one side of the phosphorylation site of $EIIA^{Ntr}$ (Fig. 1A). $EIIA^{Glc}$(E86A), a mutant in which one negatively charged amino acid was changed to alanine, can be phosphorylated by HPr; however, it completely lost the PDEMS (Fig. 1B and C), suggesting the involvement of the

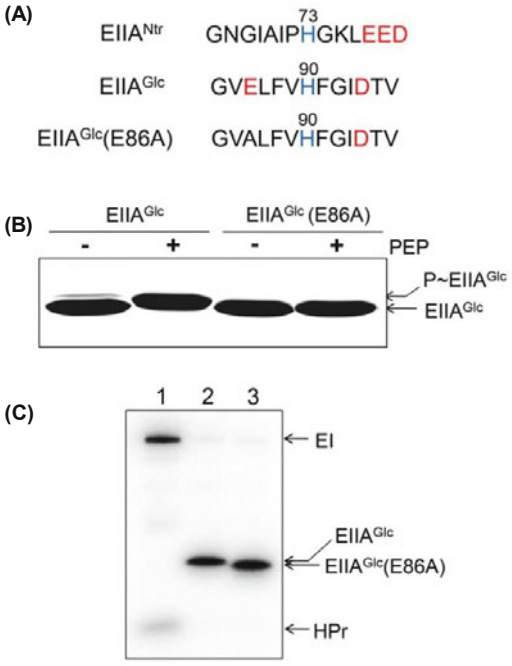

Fig. 1. Effect of a negatively charged amino acid surrounding the phosphorylation site on the PDEMS of $EIIA^{Glc}$. (A) Comparison of amino acid sequences surrounding the phosphorylation site of $EIIA^{Ntr}$ and $EIIA^{Glc}$. Negatively charged amino acids (E86 and D94) adjacent to the phosphorylation site (His-90) are symmetrically placed in $EIIA^{Glc}$, while $EIIA^{Ntr}$ has negatively charged amino acids that are placed on only one side of the phosphorylation site (H-73). (B) Loss of the PDEMS in $EIIA^{Glc}$(E86A). The phosphorylation reactions of $EIIA^{Glc}$ and $EIIA^{Glc}$(E86A) were performed in the presence of purified EI, HPr and 1 mM PEP at 37°C for 10 min. The proteins were separated by SDS-PAGE using a 4–20% gradient polyacrylamide gel and stained with Coomassie Brilliant Blue. (C) HPr-mediated phosphorylation of $EIIA^{Glc}$(E86A). The phosphorylation reactions of $EIIA^{Glc}$ and $EIIA^{Glc}$(E86A) were performed in the presence of [^{32}P] PEP (20 μM). The proteins were separated by SDS-PAGE using a 4–20% gradient polyacrylamide gel. lane 1, EI and HPr; lane 2, EI, HPr and $EIIA^{Glc}$; lane 3, EI, HPr and $EIIA^{Glc}$ (E86A). The figure was modified from Supplementary data Fig. S1 in Lee *et al.* (2013a).

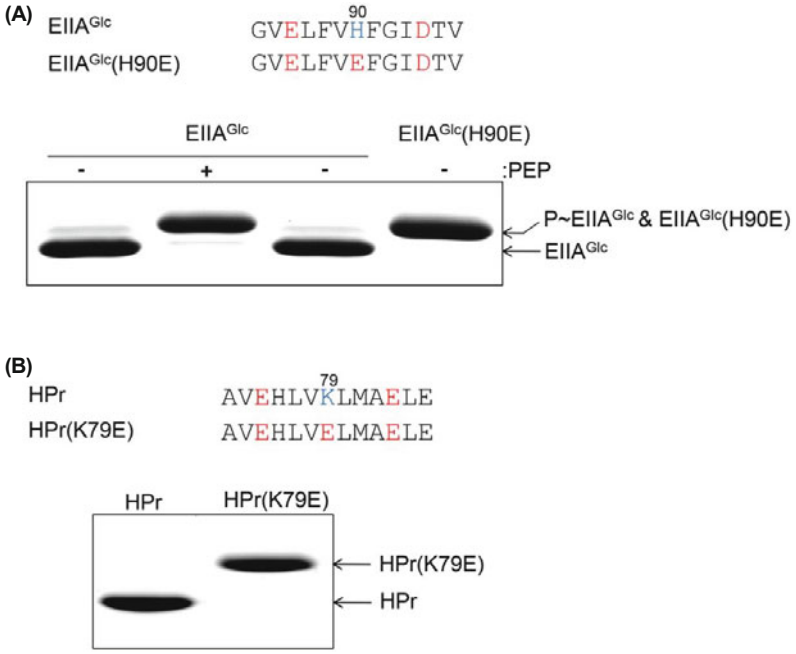

Fig. 2. Mimicry of phosphorylation by a negatively charged amino acid. (A) The electrophoretic mobility shift of phosphorylated EIIA^{Glc} and EIIA^{Glc}(H90E) during SDS-PAGE. EIIA^{Glc}(H90E) and phosphorylated EIIA^{Glc} were separated by SDS-PAGE using a 14% polyacrylamide gel, and stained with Coomassie Brilliant Blue. (B) The electrophoretic mobility shift of HPr(K79E) during SDS-PAGE. The purified proteins were separated by SDS-PAGE using a 4–20% gradient poly-acrylamide gel, and stained with Coomassie Brilliant Blue. The figure was modified from Fig. 1 in Lee *et al.* (2013b).

distribution of negatively charged amino acids surrounding the phosphorylation site in the PDEMS. Additionally, instead of phosphorylation, substitution of a histidine residue with a negatively charged amino acid glutamate can also induce the electrophoretic mobility shift (EMS) in the absence of phosphorylation (Fig. 2A). These results indicate that the negative charge introduced by phosphorylation is important for the PDEMS of the protein. This assumption is supported by the result of the EMS phenomenon in the HPr mutant K79E (Fig. 2B). Based on these results, we can predict the presence of an EMS-related motif ($\Theta X_3 \Theta X_3 \Theta$, where Θ corresponds to an acidic amino acid or phosphorylated amino acid, and X represents any amino acid).

To determine whether the number of the interval amino acids (X) is important for the EMS, several mutant proteins with 0 to 4 amino acids between the negatively charged amino

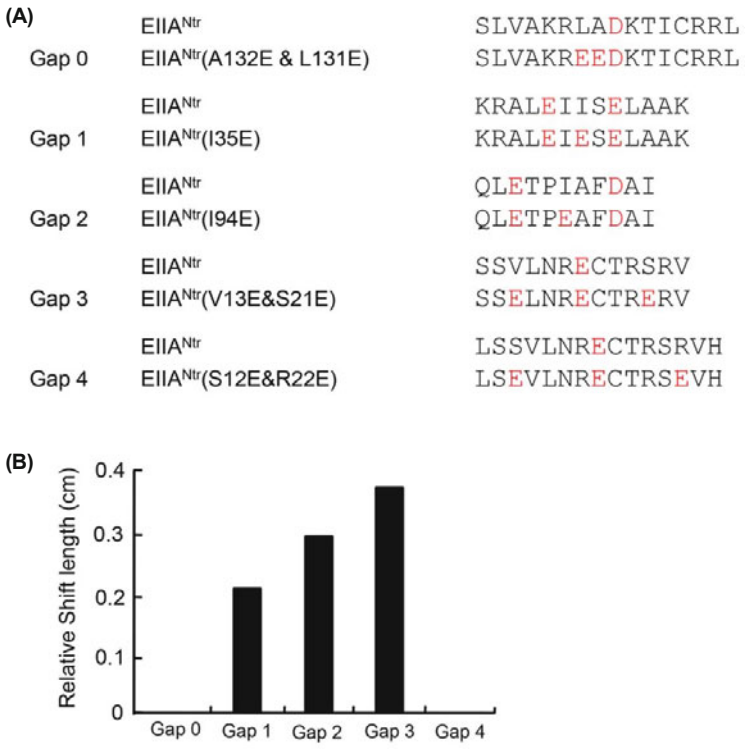

Fig. 3. Effect of the length of a gap region on the EMS of proteins during SDS-PAGE. (A) Amino acid sequences of the EMS-related motifs with various gap lengths introduced into EIIA^{Ntr} by mutation (B) The degrees of mobility shift of EIIA^{Ntr} mutant proteins. The mobility shift distances of EIIA^{Ntr} mutant proteins during SDS-PAGE were measured compared to the position of wild-type EIIA^{Ntr} on the gel. The figure was modified from Fig. 3 in Lee *et al.* (2013b).

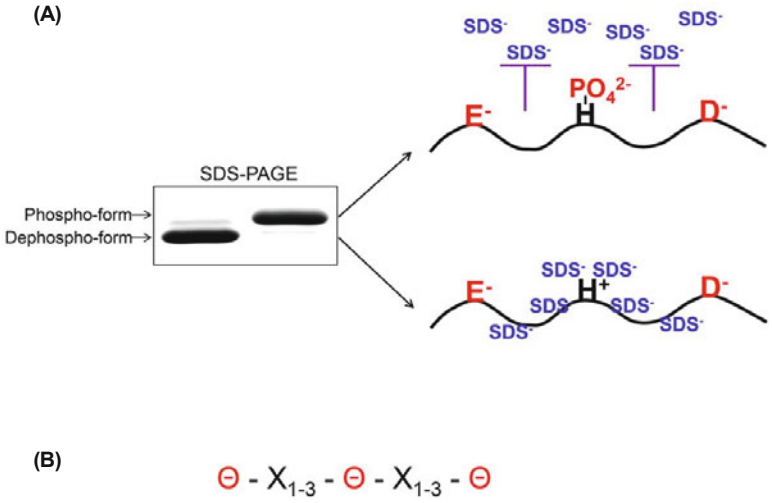

Fig. 4. Model for the PDEMS phenomenon and the EMS-related motif. (A) Molecular model for the PDEMS phenomenon. Protein phosphorylation induces the formation of the EMS-related motif which inhibits the binding of SDS to the peptide bond of proteins by charge-charge repulsion; consequently, the decreased ratio of bound SDS per protein results in the mobility shift. (B) The diagram of the EMS-related motif. Θ corresponds to a negatively charged amino acid (E or D) or phosphorylated amino acid, and X denotes any amino acid. The figure was modified from a graphic abstract in Lee *et al.* (2013b).

acids (Gaps 0–4) were constructed (Fig. 3A). Mutant proteins with 1–3 gaps showed an EMS in a gap length-dependent manner; however, those with a gap of 0 or 4 amino acids did not exhibit an EMS (Fig. 3B). Therefore, we defined the EMS-related motif as $\Theta X_{1\text{-}3}\Theta X_{1\text{-}3}\Theta$. Because the mobility of a protein during SDS-PAGE is directly affected by the number of SDS molecules bound to the protein (Rath *et al.*, 2009), the amount of SDS molecules bound to proteins was examined. Expectedly, the amount of SDS bound to HPr (K79E) via the EMS-related motif decreased significantly compared to that bound to HPr (Lee *et al.*, 2013b). In conclusion, these results suggest that a PDEMS in a protein is caused by the introduction of a negative charge by phosphorylation and consequently, the decrease in the amount of SDS molecules that bind to the protein (Fig. 4A).

Many proteins from diverse organisms show the mobility shift during SDS-PAGE when phosphorylated or mutated to contain a negatively charged amino acid, and most of them have the EMS-related motif. For example, the murine Bcl-2 family protein BAD, which shows a PDEMS, has three phosphorylation sites (Ser122, Ser136, and Ser155). The S122A and S136A double mutation hardly affects the PDEMS; however, BAD (S155A) did not exhibit a PDEMS (Zhou *et al.*, 2000). Studying the amino acid sequence of BAD shows that no negatively charged amino acids exists near S122 and S136 (within 5 residues), whereas there is the EMS-related motif fitting the consensus $\Theta X_1\Theta X_1\Theta$ near S155 (MSDEFEG, the phosphorylation residue underlined). Similar results were reported in cases of RAD51 from *Homo sapiens* (Alligand *et al.*, 2017), protein kinase C alpha type from *Rattus norvegicus* (Heckman *et al.*, 2017), ecdysoneless homolog isoform 1 from *H. sapiens* (Mir *et al.*, 2015), Tau4 from *H. sapiens* (Steiner *et al.*, 1990), IκB-α from *H. sapiens* (Imbert *et al.*, 1996), and Mer2 from *Saccharomyces cerevisiae* (Sasanuma *et al.*, 2008).

Design of a mutant protein with the EMS-related motif : Since the EMS-related motif is crucial to the PDEMS of a protein (Lee *et al.*, 2013a, 2013b), the construction of a protein showing a PDEMS requires the formation of the EMS-related motif. Based on the distribution of the negatively charged amino acids situated on both sides of the phosphorylation site, the substitution of one or two residues with a negatively charged amino acid (E or D) is required for the formation of the EMS-related motif (Fig. 4B). Because the PDEMS of a protein is caused by the insertion of the negative charge formed by phosphorylation, but not by the phosphorylation itself (Lee *et al.*, 2013a, 2013b), the position of the phosphorylation site is not critical in this design. In other words, the EMS-related motif can be formed when the phosphorylation site is located on the edges of the motif, as well as the center. Similarly, aspartate and glutamate residues seem to exhibit the same effect on the PDEMS (Lee *et al.*, 2013a, 2013b). Although an EMS-related motif with a gap of 3 amino acids induces the strongest mobility shift on SDS-PAGE (Fig. 3), the mobility shift induced by an EMS-related motif with a gap of 1 amino acid is also strong enough to distinguish two proteins during SDS-PAGE (Fig. 3). Because the distribution pattern of the negatively charged amino acids surrounding the phosphorylation site is highly diverse among various proteins, designing an EMS-related motif with a gap of 3 amino acids through only a single substitution is very rare. Substitution of the amino acid residues adjacent to the phosphorylation site, which are critical for the function of protein, could affect the function or solubility of the protein (Lee *et al.*, 2013a); thus, the number of substituted amino acids should be minimized.

A test of functionality and solubility of a mutant protein with the EMS-related motif : To evaluate the use of the mutant protein with the EMS-related motif, it is necessary to test whether it is as effective as the wild-type protein in an *in vivo* function test. Complementation tests employing the ectopic expression of the mutant protein can evaluate its functionality if there is a specific phenotype associated with the mutant defective for the target protein. Because the substitution of amino acids may significantly affect protein structure, the solubility of the mutant protein should be also tested when its purification of the mutant protein is required for the *in vitro* phosphorylation test.

Determination of the *in vivo* phosphorylation state using the mutant protein showing a PDEMS

Construction of a strain expressing the mutant protein with the EMS-related motif : To determine the *in vivo* phospho-

rylation state using the mutant protein showing a PDEMS, the construction of a strain expressing the mutant protein is required. Because over-production of proteins can induce the formation of an inclusion body, determination of the conditions for the appropriate expression of the mutant protein is important. This can be assisted by complementation tests for evaluating whether the mutant protein can act as a substitute for the wild-type protein *in vivo*.

Determination of the *in vivo* phosphorylation state : The *in vivo* phosphorylation state of the target protein is determined by western blotting analysis (Lee *et al.*, 2013a). Because the phosphorylation state can be changed even during centrifugation, it is necessary to fix the phosphorylation state of a protein of interest before cell harvesting, if possible. For example, PTS components are mostly phosphorylated during centrifugation and while replacing the medium with a solution without a sugar, they can be phosphorylated within a minute. Many bacterial proteins such as histidine kinases and PTS proteins are phosphorylated at the histidine residues: the N-1 or N-3 position of a histidine residue (Postma *et al.*, 1993). The phosphate groups attached to histidine residues, especially at the N-1 position, are known to be very unstable at acidic and neutral pHs (Hultquist, 1968). Therefore, in this case, a quenching process is required to fix the phosphorylation state of the target protein (Park *et al.*, 2013). A strong alkaline solution can disrupt cells in seconds without the need for cell harvesting and stabilize the phosphohistidine, although phospho-serine, threonine, and tyrosine are more stable at acidic pHs. After the growth of the strain expressing the mutant protein to an appropriate phase, an aliquot (0.2 ml) of the cell culture is quenched by mixing it with 20 µl of 5 M NaOH. After vortexing for 10 sec, 80 µl of 3 M sodium acetate (pH 5.2) and 0.9 ml of ethanol are added. After incubation at -70°C for 15–60 min (phospho-HPr is gradually dephosphorylated even at high pHs), the samples are centrifuged at 4°C for 10 min. The pellet is washed with 70% ethanol and resuspended in 100 µl of SDS sample buffer. Then, a 20 µl-volume of the sample is immediately subjected to SDS-PAGE without boiling. Boiling will significantly decrease the pH of the Tris buffer and hydrolyze phosphohistidine.

Materials

Reagents

- LB broth: 1% tryptone, 0.5% yeast extract, 1% NaCl
- LB plate: 1% tryptone, 0.5% yeast extract, 1% NaCl, 1.5% Bacto-agar
- Phosphorylation reaction buffer: 1 mM PEP, 0.1 M Tris·HCl (pH 7.5), 2 mM $MgCl_2$, 1 mM EDTA, 10 mM KCl, 0.5 mM dithiothreitol
- Binding buffer: 20 mM HEPES-KOH (pH 8.0), 200 mM NaCl
- Elution buffer: 20 mM HEPES-KOH, 300 mM NaCl, 200 mM imidazole
- SDS-PAGE sample buffer: 250 mM Tris·HCl (pH 6.8), 10% glycerol, 1% SDS, 1% 2-mercaptoethanol
- Pfu DNA polymerase (Enzynomics)
- *Dpn*I (New England BioLabs)
- 3 M sodium acetate (pH 5.2)
- NaOH
- 70% Ethanol

Equipment

- 1.5 ml microcentrifuge tube (Sarstedt)
- Q-Cycler (Quanta Biotech)
- MicroPulser electroporator (Bio-Rad)
- Incubator (Hanbaek)
- 4–20% gradient or 14% acrylamide gel
- TALON metal affinity resin (BD Biosciences Clontech)
- PVDF membrane (Immobilin-P, Millipore)
- HiLoad 16/60 Superdex 75 (GE Healthcare)
- Centrifuge (Eppendorf)

Protocols

A. Design and construction of a mutant protein with the EMS-related motif

1. Select the amino acid residue(s) for the construction of a mutant protein with the EMS-related motif and design the mutagenic primers for the substitution of the amino acid residue(s) with an aspartate or glutamate residue.
   - ► **NOTE:** The EMS-related motif can be formed when the phosphorylation site is located on the edges of the motif as well as the center.
   - ► **NOTE:** The number of substituted amino acids should be minimized.
2. Amplify the plasmid with the altered codon by performing 20–30 rounds of PCR with the mutagenic primers.
3. Treat the PCR product with *Dpn*I to degrade the methylated wild-type DNA used as a template.
4. Transform *E. coli* cells with the treated DNA and spread the transformed cells on an LB plate containing antibiotics.
5. Check the mutation by sequencing the plasmid DNA from several clones.

B. Test of the functionality of a mutant protein with the EMS-related motif

1. Construct a mutant strain in which the target gene in the chromosome is deleted and which expresses the wild-type or mutant protein in trans.
2. Compare the phenotypes of the wild-type strain and the mutant strain expressing the wild-type or mutant protein.
   - ► **NOTE:** The levels of proteins expressed in the plasmids should be as similar as possible to those of the target protein expressed in the chromosome.
   - ► **NOTE:** The mutant protein may be considered to be functional if the degree of complementation of the mutant protein is similar to that of the wild-type protein.

C. Determination of the *in vitro* phosphorylation state, with an example of bacterial PTS proteins

1. Prepare *E. coli* cells overproducing the His-tagged recombinant mutant protein and resuspend cells with the binding buffer.
2. Lyse the cells using a French pressure cell at 12,000 psi and remove the cell debris by centrifugation at 12,000 × *g*

for 20 min at 4°C.
3. Load the supernatant into a metal affinity resin and gently rotate the column for 20 min at 4°C.
4. Wash the column with the binding buffer at least thrice and elute the proteins bound to the affinity resin using the elution buffer.
5. Remove the imidazole and contaminated proteins by gel-filtration chromatography and store the purified proteins at -80°C until use.
6. Perform the *in vitro* phosphorylation reactions with the purified proteins in the presence of 20 μl of the phosphorylation reaction buffer at 37°C for 1 min.
7. Stop the phosphorylation reaction by the addition of 5 μl of SDS-PAGE sample buffer and analyze the proteins by SDS-PAGE.

► **NOTE:** Boiling of the samples before SDS-PAGE should be avoided. Phosphorylation on histidine, glutamic acid, aspartic acid, arginine, cysteine, and lysine is very labile and can be easily destroyed by boiling (Mann *et al.*, 2002).

D. Determination of the *in vivo* phosphorylation state

1. Culture the mutant strain that is defective for the target protein and harbors the plasmid expressing the mutant protein to the mid-logarithmic phase.
2. An aliquot (0.2 ml) of the cell culture is mixed with 20 μl of 5 M NaOH. After vortexing for 10 sec, 80 μl of 3 M sodium acetate (pH 5.2) and 0.9 ml of ethanol are added. After incubation at -70°C for 15–60 min, the samples are centrifuged at 4°C for 10 min. The pellet is washed with 70% ethanol to remove the excessive salts.

► **NOTE:** The phosphate groups attached to histidine residues, especially at the N-1 position, are known to be very unstable at acidic and neutral pHs (Hultquist, 1968). In this case, to fix the phosphorylation state of the target protein, an aliquot (0.2 ml) of the cell culture is quenched by mixing it with 20 μl of 5 M NaOH. Prolonged incubation of the samples will gradually dephosphorylate phospho-histidine even at -70°C.

3. After the pellet is resuspended in 100 μl of SDS sample buffer, it is immediately run on an SDS-PAGE gel, and the separated proteins are transferred onto a PVDF membrane.
4. Develop the target protein by immunoblotting using antibodies against the target protein.

Expected results

Unlike $EIIA^{Glc}$ of the glucose PTS, $EIIA^{Ntr}$ of the nitrogen PTS does not show a PDEMS. To make a mutant protein with an EMS-related motif with a gap of 3 amino acids, an isoleucine residue at a position 69 was substituted with an aspartate residue (Fig. 5A). $EIIA^{Ntr}$ (I69D) clearly exhibits a PDEMS (Fig. 5B), but this protein was insoluble (it formed inclusion bodies) and was not as phosphorylatable as the wild-type protein (Lee *et al.*, 2013a). Fortunately, $EIIA^{Ntr}$ (K75D) with an EMS-related motif with a gap of 1 amino acid showed a PDEMS and was as phosphorylatable as the wild-type protein (Fig. 5B). Additionally, the expression of $EIIA^{Ntr}$(K75D) restored the phenotype of the mutant strain defective for $EIIA^{Ntr}$, to a level similar to that in the case of the wild-type protein (Lee *et al.*, 2013a), suggesting that $EIIA^{Ntr}$(K75D) can replace the wild-type protein *in vivo*. Therefore, we used $EIIA^{Ntr}$(K75D) as a protein for the determination of the *in vitro* and *in vivo* phosphorylation states of $EIIA^{Ntr}$.

Using purified $EIIA^{Ntr}$(K75D), we tested the possibility that an amino acid might affect the phosphorylation state of $EIIA^{Ntr}$. Among the 20 amino acids tested, only the addition of glutamine clearly inhibited the phosphorylation of $EIIA^{Ntr}$(K75D) (Lee *et al.*, 2013a). Further experiments using purified $EIIA^{Ntr}$(K75D) revealed the inhibitory effect of glutamine and the stimulatory effect of α-ketoglutarate (Fig. 6A).

The *in vivo* phosphorylation test of $EIIA^{Ntr}$ was performed in the *E. coli* strain that is defective for $EIIA^{Ntr}$ and ectopically expresses $EIIA^{Ntr}$(K75D). $EIIA^{Ntr}$(K75D) in cells grown in LB medium existed mostly in a phosphorylated form; however, only its dephosphorylated form was detected in the mutant strain defective for EI^{Ntr}, a component of the nitrogen PTS necessary for the phosphorylation of $EIIA^{Ntr}$ (Lee *et al.*, 2013a). These results indicate that $EIIA^{Ntr}$(K75D) effectively acts as an *in vivo* phosphorylation-state probe of $EIIA^{Ntr}$. Because intracellular α-ketoglutarate and glutamine levels reflect cellular nitrogen availability (Bahr *et al.*, 2011), the change of the phosphorylation state of $EIIA^{Ntr}$(K75D) according to nitrogen availability was measured. Most $EIIA^{Ntr}$(K75D) existed in a dephosphorylated form in cells grown in the presence of ammonium salts, which are a good nitro-

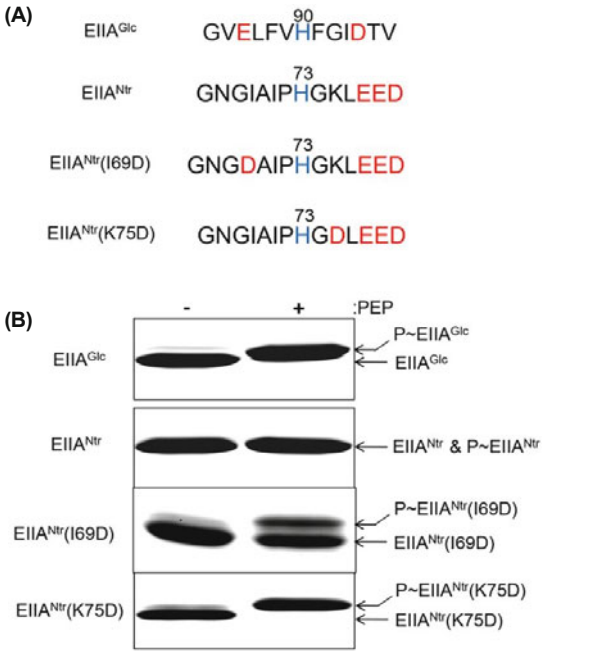

Fig. 5. Construction of mutant $EIIA^{Ntr}$ proteins showing a PDEMS. (A) Comparison of amino acid sequences surrounding the phosphorylation sites of $EIIA^{Glc}$, $EIIA^{Ntr}$, $EIIA^{Ntr}$(I69D), and $EIIA^{Ntr}$(K75D). (B) The PDEMS of $EIIA^{Ntr}$(I69D) and $EIIA^{Ntr}$(K75D). The phosphorylation reactions of $EIIA^{Ntr}$, $EIIA^{Ntr}$(I69D), and $EIIA^{Ntr}$(K75D) were performed in the presence of purified EI^{Ntr}, NPr, and 1 mM PEP at 37°C for 10 min. The proteins were separated by SDS-PAGE using a 14% gradient polyacrylamide gel, and stained with Coomassie Brilliant Blue. The figure was modified from Fig. 1 in Lee *et al.* (2013a).

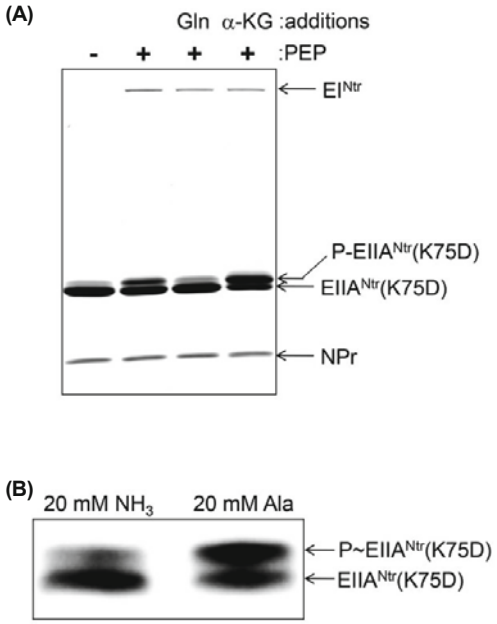

Fig. 6. Application of the mutant protein showing a PDEMS to search for signaling molecules regulating the nitrogen PTS. (A) Regulation of the *in vitro* phosphorylation of $EIIA^{Ntr}$(K75D) by glutamine and α-ketoglutarate. The phosphorylation reaction of $EIIA^{Ntr}$(K75D) was performed in the presence of PEP, EI^{Ntr}, and NPr. Glutamine (Gln) and α-ketoglutarate (α-KG) were added at a concentration of 5 mM when required. After incubation for 1 min at room temperature, the phosphorylation reactions were stopped by the addition of SDS-PAGE sample buffer and the proteins were separated by 14% SDS-PAGE. (B) Determination of the *in vivo* phosphorylation state of $EIIA^{Ntr}$(K75D). The mutant strain defective for $EIIA^{Ntr}$ and harboring the plasmid expressing $EIIA^{Ntr}$(K75D) was grown to the mid-logarithmic phase in W salts medium containing 0.2% glucose with 20 mM $(NH_4)_2SO_4$ or alanine. The samples were quenched using 5 M NaOH and processed as described in the protocols above, and were separated on 14% SDS-PAGE gels and analyzed by western blotting. The figure was modified from Figs. 2 and 3 in Lee *et al.* (2013a).

gen source; on the contrary, the amount of the phosphorylated form significantly increased in the presence of the same concentration of alanine, a poor nitrogen source (Fig. 6B). Further experiments showed that the phosphorylation of the nitrogen PTS is regulated in response to nitrogen availability (Lee *et al.*, 2013a). Since then, similar results were reported in diverse proteobacteria, including *Salmonella enterica* serovar Typhimurium (Yoo *et al.*, 2016), *Sinorhizobium meliloti* (Goodwin and Gage, 2014), and *Caulobacter crescentus* (Ronneau *et al.*, 2016).

$EIIA^{Ntr}$(K75D), the mutant protein showing a PDEMS was used to identify the signal molecules controlling the phosphorylation state of the nitrogen PTS; this validates the use of this method as a tool to construct a probe for exploring the phosphorylation state of the target protein. Our method was successfully applied to $EIIA^{Ntr}$ of *S.* Typhimurium (Yoo *et al.*, 2016). *Salmonella* $EIIA^{Ntr}$ with an EMS-related motif also exhibited a PDEMS, and its dephosphorylated form increased in the presence of glutamine. Therefore, our protocol for desinging a protein that shows a PDEMS without affecting its activity can simplify studies regarding the *in vitro* and *in vivo* phosphorylation states of signal transduction proteins from various organisms

Acknowledgements

This work was supported by research grants from the Bio & Medical Technology Development Program of the NRF funded by the MSIT (number NRF-2017M3A9E4078017); the NRF funded by the Ministry of Science and ICT (NRF-2018R1A1A1A05023049 and NRF-2018R1A5A1025077). Huitae Min was supported by the BK21 plus program of the NRF, Republic of Korea.

Conflict of Interest

The authors declare that they have no conflicts of financial interests.

References

Alligand, B., Le Breton, M., Marquis, D., Vallette, F., and Fleury, F. 2017. Functional effects of diphosphomimetic mutations at cAbl-mediated phosphorylation sites on Rad51 recombinase activity. *Biochimie* **139**, 115–124.

Bahr, T., Luttmann, D., Marz, W., Rak, B., and Gorke, B. 2011. Insight into bacterial phosphotransferase system-mediated signaling by interspecies transplantation of a transcriptional regulator. *J. Bacteriol.* **193**, 2013–2026.

Bai, J., Zhao, Y., Wang, Z., Liu, C., Wang, Y., and Li, Z. 2013. Dual-readout fluorescent assay of protein kinase activity by use of TiO_2-coated magnetic microspheres. *Anal. Chem.* **85**, 4813–4821.

Cohen, P. 2002a. The origins of protein phosphorylation. *Nat. Cell Biol.* **4**, E127–130.

Cohen, P. 2002b. Protein kinases--the major drug targets of the twenty-first century? *Nat. Rev. Drug Discov.* **1**, 309–315.

Deutscher, J., Francke, C., and Postma, P.W. 2006. How phosphotransferase system-related protein phosphorylation regulates carbohydrate metabolism in bacteria. *Microbiol. Mol. Biol. Rev.* **70**, 939–1031.

Goodwin, R.A. and Gage, D.J. 2014. Biochemical characterization of a nitrogen-type phosphotransferase system reveals that enzyme EI^{Ntr} integrates carbon and nitrogen signaling in *Sinorhizobium meliloti*. *J. Bacteriol.* **196**, 1901–1907.

Heckman, C.A., Pandey, P., Cayer, M.L., Biswas, T., Zhang, Z.Y., and Boudreau, N.S. 2017. The tumor promoter-activated protein kinase Cs are a system for regulating filopodia. *Cytoskeleton (Hoboken)* **74**, 297–314.

Hogema, B.M., Arents, J.C., Bader, R., Eijkemans, K., Yoshida, H., Takahashi, H., Aiba, H., and Postma, P.W. 1998. Inducer exclusion in *Escherichia coli* by non-PTS substrates: the role of the PEP to pyruvate ratio in determining the phosphorylation state of enzyme IIA^{Glc}. *Mol. Microbiol.* **30**, 487–498.

Hultquist, D.E. 1968. The preparation and characterization of phosphorylated derivatives of histidine. *Biochim. Biophys. Acta* **153**, 329–340.

Imbert, V., Rupec, R.A., Livolsi, A., Pahl, H.L., Traenckner, E.B., Mueller-Dieckmann, C., Farahifar, D., Rossi, B., Auberger, P., Baeuerle, P.A., *et al.* 1996. Tyrosine phosphorylation of IκB-α activates NF-κB without proteolytic degradation of IκB-α. *Cell* **86**, 787–798.

Inagaki, M., Inagaki, N., Takahashi, T., and Takai, Y. 1997. Phosphorylation-dependent control of structures of intermediate filaments: a novel approach using site- and phosphorylation state-specific antibodies. *J. Biochem.* **121**, 407–414.

Inamori, K., Kyo, M., Nishiya, Y., Inoue, Y., Sonoda, T., Kinoshita, E., Koike, T., and Katayama, Y. 2005. Detection and quantifica-

tion of on-chip phosphorylated peptides by surface plasmon resonance imaging techniques using a phosphate capture molecule. *Anal. Chem.* **77**, 3979–3985.

Ji, L., Wu, J.H., Luo, Q., Li, X., Zheng, W., Zhai, G., Wang, F., Lu, S., Feng, Y.Q., Liu, J., *et al.* 2012. Quantitative mass spectrometry combined with separation and enrichment of phosphopeptides by titania coated magnetic mesoporous silica microspheres for screening of protein kinase inhibitors. *Anal. Chem.* **84**, 2284–2291.

Kaufmann, H., Bailey, J.E., and Fussenegger, M. 2001. Use of antibodies for detection of phosphorylated proteins separated by two-dimensional gel electrophoresis. *Proteomics* **1**, 194–199.

Kinoshita, E., Kinoshita-Kikuta, E., and Koike, T. 2009. Separation and detection of large phosphoproteins using Phos-tag SDS-PAGE. *Nat. Protoc.* **4**, 1513–1521.

Kinoshita, E., Kinoshita-Kikuta, E., and Koike, T. 2017. Zn(II)-Phos-tag SDS-PAGE for separation and detection of a DNA damage-related signaling large phosphoprotein. *Methods Mol. Biol.* **1599**, 113–126.

Lee, V.M., Goedert, M., and Trojanowski, J.Q. 2001. Neurodegenerative tauopathies. *Annu. Rev. Neurosci.* **24**, 1121–1159.

Lee, J.K. and Kim, N.J. 2017. Recent advances in the inhibition of p38 MAPK as a potential strategy for the treatment of Alzheimer's disease. *Molecules* **22**, 1287.

Lee, C.R., Park, Y.H., Kim, M., Kim, Y.R., Park, S., Peterkofsky, A., and Seok, Y.J. 2013a. Reciprocal regulation of the autophosphorylation of enzyme I^{Ntr} by glutamine and α-ketoglutarate in *Escherichia coli*. *Mol. Microbiol.* **88**, 473–485.

Lee, C.R., Park, Y.H., Kim, Y.R., Peterkofsky, A., and Seok, Y.J. 2013b. Phosphorylation-dependent mobility shift of proteins on SDS-PAGE is due to decreased binding of SDS. *Bull. Korean Chem. Soc.* **34**, 2063–2066.

Li, T., Liu, D., and Wang, Z. 2009. Microarray-based Raman spectroscopic assay for kinase inhibition by gold nanoparticle probes. *Biosens. Bioelectron.* **24**, 3335–3339.

Mann, M., Ong, S.E., Gronborg, M., Steen, H., Jensen, O.N., and Pandey, A. 2002. Analysis of protein phosphorylation using mass spectrometry: deciphering the phosphoproteome. *Trends Biotechnol.* **20**, 261–268.

Manning, G., Plowman, G.D., Hunter, T., and Sudarsanam, S. 2002. Evolution of protein kinase signaling from yeast to man. *Trends Biochem. Sci.* **27**, 514–520.

Mir, R.A., Bele, A., Mirza, S., Srivastava, S., Olou, A.A., Ammons, S.A., Kim, J.H., Gurumurthy, C.B., Qiu, F., Band, H., *et al.* 2015. A novel interaction of Ecdysoneless (ECD) protein with R2TP complex component RUVBL1 is required for the functional role of ECD in cell cycle progression. *Mol. Cell Biol.* **36**, 886–899.

Park, Y.H., Lee, C.R., Choe, M., and Seok, Y.J. 2013. HPr antagonizes the anti-σ^{70} activity of Rsd in *Escherichia coli*. *Proc. Natl. Acad. Sci. USA* **110**, 21142–21147.

Postma, P.W., Lengeler, J.W., and Jacobson, G.R. 1993. Phosphoenolpyruvate:carbohydrate phosphotransferase systems of bacteria. *Microbiol. Rev.* **57**, 543–594.

Rath, A., Glibowicka, M., Nadeau, V.G., Chen, G., and Deber, C.M. 2009. Detergent binding explains anomalous SDS-PAGE migration of membrane proteins. *Proc. Natl. Acad. Sci. USA* **106**, 1760–1765.

Ronneau, S., Petit, K., De Bolle, X., and Hallez, R. 2016. Phosphotransferase-dependent accumulation of (p)ppGpp in response to glutamine deprivation in *Caulobacter crescentus*. *Nat. Commun.* **7**, 11423.

Sasanuma, H., Hirota, K., Fukuda, T., Kakusho, N., Kugou, K., Kawasaki, Y., Shibata, T., Masai, H., and Ohta, K. 2008. Cdc7-dependent phosphorylation of Mer2 facilitates initiation of yeast meiotic recombination. *Genes Dev.* **22**, 398–410.

Steiner, B., Mandelkow, E.M., Biernat, J., Gustke, N., Meyer, H.E., Schmidt, B., Mieskes, G., Soling, H.D., Drechsel, D., Kirschner, M.W., *et al.* 1990. Phosphorylation of microtubule-associated protein tau: identification of the site for Ca^{2+}-calmodulin dependent kinase and relationship with tau phosphorylation in Alzheimer tangles. *EMBO J.* **9**, 3539–3544.

Takeda, H., Goshima, N., and Nomura, N. 2010. High-throughput kinase assay based on surface plasmon resonance. *Methods Mol. Biol.* **627**, 131–145.

Wang, Z., Lee, J., Cossins, A.R., and Brust, M. 2005. Microarray-based detection of protein binding and functionality by gold nanoparticle probes. *Anal. Chem.* **77**, 5770–5774.

Wang, Z., Levy, R., Fernig, D.G., and Brust, M. 2006. Kinase-catalyzed modification of gold nanoparticles: a new approach to colorimetric kinase activity screening. *J. Am. Chem. Soc.* **128**, 2214–2215.

Wang, Y., Zhang, L., Liang, R.P., Bai, J.M., and Qiu, J.D. 2013. Using graphene quantum dots as photoluminescent probes for protein kinase sensing. *Anal. Chem.* **85**, 9148–9155.

Xu, X., Liu, X., Nie, Z., Pan, Y., Guo, M., and Yao, S. 2011. Label-free fluorescent detection of protein kinase activity based on the aggregation behavior of unmodified quantum dots. *Anal. Chem.* **83**, 52–59.

Yoo, W., Yoon, H., Seok, Y.J., Lee, C.R., Lee, H.H., and Ryu, S. 2016. Fine-tuning of amino sugar homeostasis by $EIIA^{Ntr}$ in *Salmonella* Typhimurium. *Sci. Rep.* **6**, 33055.

Zhao, Z., Zhou, X., and Xing, D. 2012. Highly sensitive protein kinase activity assay based on electrochemiluminescence nanoprobes. *Biosens. Bioelectron.* **31**, 299–304.

Zhou, X.M., Liu, Y., Payne, G., Lutz, R.J., and Chittenden, T. 2000. Growth factors inactivate the cell death promoter BAD by phosphorylation of its BH3 domain on Ser155. *J. Biol. Chem.* **275**, 25046–25051.

Zhou, J., Xu, X., Liu, W., Liu, X., Nie, Z., Qing, M., Nie, L., and Yao, S. 2013. Graphene oxide-peptide nanocomplex as a versatile fluorescence probe of protein kinase activity based on phosphorylation protection against carboxypeptidase digestion. *Anal. Chem.* **85**, 5746–5754.

Zschiedrich, C.P., Keidel, V., and Szurmant, H. 2016. Molecular mechanisms of two-component signal transduction. *J. Mol. Biol.* **428**, 3752–3775.